IOPscience iopscience.iop.org

Home Search Collections Journals About Contact us My IOPscience

Freezing of a quantum hard-sphere liquid at zero temperature: a density-functional approach

This article has been downloaded from IOPscience. Please scroll down to see the full text article.

1991 J. Phys.: Condens. Matter 3 593

(http://iopscience.iop.org/0953-8984/3/5/008)

View the table of contents for this issue, or go to the journal homepage for more

Download details:
IP Address: 171.66.16.151
The article was downloaded on 11/05/2010 at 07:05

Please note that terms and conditions apply.

J. Phys.: Condens. Matter 3 (1991) 593–607. Printed in the UK

Freezing of a quantum hard-sphere liquid at zero temperature: a density-functional approach

A R Denton, P Nielaba†, K J Runge and N W Ashcroft

Laboratory of Atomic and Solid State Physics and Materials Science Center, Cornell University, Ithaca, NY 14853-2501, USA

Received 26 June 1990

Abstract. Quantum freezing of the ground-state Bose hard-sphere liquid is described by an extension of the classical density-functional method, in the form of the modified weighted-density approximation, to non-uniform *quantum* liquids at zero temperature. As input, the theory requires only structural and thermodynamic information for the *uniform* quantum liquid, this being obtained from the paired phonon analysis. Results for the solid-phase energies and freezing parameters of FCC, HCP, and BCC crystal structures are in generally good agreement with available simulation data, and are quite insensitive to the crystal structure. An analogous extension of the Ramakrishnan–Yussouff second-order approximation leads to freezing parameters in generally poorer agreement with simulation.

1. Introduction

In recent years the density-functional method [1], in a variety of formulations, has been widely applied to phenomena involving non-uniform *classical* liquids. A fundamental application has been to the freezing transition in simple liquids, in which the solid phase is treated as an extremely non-uniform liquid. Using information on the structure and thermodynamics of the *uniform* liquid, the method leads to predictions for the densities of the coexisting liquid and solid phases, the latent heat of transition, and the Lindemann parameter. Although agreement with simulation tends to vary with the system studied and with the version of the method used, especially notable success has been obtained in the case of the *classical hard-sphere* system, where the predicted freezing parameters agree with simulation usually to within a few percent [1]. This is a particularly important success since the hard-sphere system may be used as a reference system in perturbation theory studies of more realistic systems [2]. Although there have been numerous applications of the density-functional method to freezing of other classical liquids, to date comparatively few studies have been devoted to *quantum* liquids. An important issue, then, is the manner in which the general method may be extended from classical to quantum systems, and whether, in particular, it can illuminate the physical nature of the freezing transition in quantum liquids.

Recently, one version of the density-functional method, based on the Ramakrishnan–Yussouff (RY) second-order approximation [3], has been extended [4–6]

† Present address: Fachbereich Physik, Institut für Physik, Johannes Gutenberg Universität Mainz, Staudinger Weg 7, D-6500 Mainz, Germany.

0953-8984/91/050593+15$03.50 © 1991 IOP Publishing Ltd

and applied to freezing of a Lennard-Jones model of ^{4}He at finite temperatures [4], and to freezing (Wigner crystallization) of the ground-state Fermi one-component plasma [5]. The purposes of this paper are three-fold: first, to describe a general extension of a quite different version of the density-functional method, based on the modified weighted-density approximation [7,8] (MWDA), from classical systems to quantum systems at zero temperature; second, to demonstrate its utility by applying it to the freezing of a Bose liquid of *hard spheres*; and third, to compare its predictions for the freezing parameters with simulation data and with the corresponding predictions of the RY second-order approximation.

The remainder of the paper is organized as follows. In section 2 we describe a straightforward extension of the MWDA to ground-state quantum systems. In section 3 we outline the computation—by means of the paired phonon analysis [9]—of the liquid-state information required as input to the theory. In section 4 we describe the application of the MWDA, as well as of the RY second-order approximation, to freezing of the Bose hard-sphere liquid, and report results for freezing into FCC, HCP, and BCC crystal structures. In section 5 we compare the results with available simulation data, and discuss implications of the theory for the nature of quantum freezing transitions. Finally, in section 6 we summarize and suggest the desirability of further studies on improving the accuracy of the liquid-state input. A preliminary report of this work has been presented elsewhere [10].

2. Density-functional method

In a density-functional approach to non-uniform quantum liquids at zero temperature the central quantity of interest is the total ground-state energy $E[\rho]$, a *unique* functional of the (spatially-varying) density $\rho(\boldsymbol{r})$, and a quantity which attains a minimum value (for constant average density) at the equilibrium density [11]. In the absence of an external potential, $E[\rho]$ can be conveniently separated into two contributions by writing

$$E[\rho] = E_{\mathrm{id}}[\rho] + E_{\mathrm{c}}[\rho] \tag{1}$$

where $E_{\mathrm{id}}[\rho]$ is the ideal-gas energy, the energy of the non-uniform system without interactions, and $E_{\mathrm{c}}[\rho]$ is the correlation energy, arising from internal interactions and exchange. The advantage of this separation is that $E_{\mathrm{id}}[\rho]$ can be treated exactly (see section 4). In contrast, $E_{\mathrm{c}}[\rho]$ is unknown for non-uniform systems and must be approximated.

The approximation for $E_{\mathrm{c}}[\rho]$ described below is a straightforward extension to non-uniform ground-state quantum liquids of the modified weighted-density approximation [7] (MWDA). The resulting quantum formulation closely parallels the classical formulation described in [7]. Its basis is the assumption that the average correlation energy per particle of the *non-uniform* system can be equated to its counterpart for the *uniform* liquid evaluated at a spatially-constant weighted density, which is further assumed to depend on a weighted average over the volume of the system of the spatially-varying physical density. The statement of the MWDA is then

$$E_c^{\mathrm{MWDA}}[\rho]/N \equiv \epsilon(\hat{\rho}) \tag{2}$$

where N is the number of particles, ϵ the uniform-liquid correlation energy per particle, and where $\hat{\rho}$ is an effective or *weighted* density, defined by

$$\hat{\rho} \equiv \frac{1}{N} \int \mathrm{d}\boldsymbol{r} \rho(\boldsymbol{r}) \int \mathrm{d}\boldsymbol{r}' \rho(\boldsymbol{r}') w(\boldsymbol{r} - \boldsymbol{r}'; \hat{\rho}). \tag{3}$$

As in the classical formulation [7, 8], the *self-consistent* choice of the density argument $\hat{\rho}$ of the 'weight function' w in (3) is an essential feature of the approximation. To ensure that the approximation is exact in the limit of a uniform liquid $[\rho(\boldsymbol{r}) \to \rho]$ the weight function must be normalized, according to

$$\int \mathrm{d}\boldsymbol{r}' w(\boldsymbol{r} - \boldsymbol{r}'; \rho) = 1. \tag{4}$$

A *unique* determination of w follows from requiring that $E_{\mathrm{c}}^{\mathrm{MWDA}}[\rho]$ satisfies the relation

$$\lim_{\rho(\boldsymbol{r}) \to \rho} \left(\frac{\delta^2 E_{\mathrm{c}}[\rho]}{\delta\rho(\boldsymbol{r})\delta\rho(\boldsymbol{r}')} \right) = v(|\boldsymbol{r} - \boldsymbol{r}'|; \rho) \tag{5}$$

where $v(|\boldsymbol{r} - \boldsymbol{r}'|; \rho)$ is now to be interpreted as an extension to quantum liquids of the classical Ornstein–Zernike direct correlation function (DCF). This requirement ensures that—to the extent that ϵ and v are known exactly for the liquid—a functional Taylor series expansion of $E_{\mathrm{c}}^{\mathrm{MWDA}}[\rho]$ about the density of a uniform reference liquid is 'exact' to second order and also includes a subset of exact higher-order terms, specifically, those terms which depend only on derivatives of v with respect to density (see [7, 8] for a more complete discussion). By now substituting the correlation energy (2) and weighted density (3) into (5), and making use of the normalization condition (4), it is straightforward to show that the weight function is given (in Fourier space) by the simple relation

$$w(k; \rho) = \frac{1}{2\epsilon'(\rho)} \left[v(k, \rho) - \delta_{k,0} \rho \epsilon''(\rho) \right] \tag{6}$$

where primes on ϵ denote derivatives with respect to density. We note, from (4) and (6), that

$$v(k = 0, \rho) = 2\epsilon'(\rho) + \rho\epsilon''(\rho) = m c_{\mathrm{l}}^2 \tag{7}$$

which may be interpreted as a 'quantum compressibility rule', with m the mass of a particle and c_{l} the speed of longitudinal sound.

Together, (2), (3), and (6) constitute the extension of the MWDA to non-uniform *quantum* liquids at zero temperature. We emphasize that as input the theory requires only the correlation energy per particle and DCF of the uniform quantum liquid.

3. Liquid-state input

For the Bose hard-sphere system, the required liquid-state information has been obtained from the paired phonon analysis [9] (PPA). This takes a trial ground-state wavefunction of the Jastrow form

$$\psi_T(\boldsymbol{r}_1, \ldots, \boldsymbol{r}_N) = \prod_{(i,j)} \mathrm{e}^{-u(r_{ij})} \tag{8}$$

and determines the pseudopotential $u(r)$ by minimization of the total ground-state energy according to

$$\frac{\delta}{\delta u(r)}\left[\frac{\langle\psi_T|H|\psi_T\rangle}{\langle\psi_T|\psi_T\rangle}\right]=0 \tag{9}$$

where, for our purposes, H is the Bose hard-sphere Hamiltonian. Two constraints are imposed on the form of $u(r)$: first, that $u(r)\to 0$ as $r\to\infty$, and second (for hard spheres), that $u(r)\to\infty$ as $r\to\sigma$, where σ denotes the hard-sphere diameter. To determine $u(r)$ the PPA exploits the formal correspondence between the quantum probability density $|\psi_T|^2$ and the classical Boltzmann factor [12], where $u(r)$ now plays the role of a classical pair potential (hence the name 'pseudopotential'). For a given $u(r)$ the corresponding radial distribution function $g(r,[u])$ may then be determined by solving one of the approximate integral equations from the theory of *classical* liquids. Because $u(r)$ turns out to be a relatively soft function of r [13–15], we have used the hypernetted chain (HNC) integral equation approximation [2]. Once $g(r,[u])$ is thus found, the correlation energy can be computed from [9, 12]

$$E_c(\rho)=\frac{\hbar^2}{4m}\rho\int \mathrm{d}r g(r,[u])\nabla^2 u(r) \tag{10}$$

and the random phase approximation then used to determine the *change* in pseudopotential $\Delta u(r)$ which gives rise to the lowest energy. Finally, $\Delta u(r)$ is added to $u(r)$ and the entire procedure repeated until the energy can no longer be lowered.

Although the PPA involves certain approximations, it nevertheless has been shown [16] to give excellent pseudopotentials $u(r)$. The method can be tested by using the PPA $u(r)$ in a Monte Carlo simulation to compute the energy. Such a test has been performed for the case of liquid ^{4}He, resulting in the lowest energy so far found [16] for a wavefunction in the form of (8). In addition, the PPA gives approximations both for the correlation energy (10) and for $g(r)$. Figure 1(a) illustrates the corresponding structure factor $S(k)$ (the Fourier transform of $g(r)-1$). From $S(k)$, we then obtain the required $v(k)$ from the simple relation [17]

$$v(k)=\frac{\hbar^2k^2}{4m}\left(\frac{1}{S^2(k)}-1\right). \tag{11}$$

It is interesting to note that this form for $v(k)$ can also be written as

$$v(k)=k_{\mathrm{B}}T\rho c(k)a(k) \tag{12}$$

where $c(k)$ is the classical direct correlation function corresponding to $S(k)$ and $a(k)\equiv(\hbar^2k^2/4mk_{\mathrm{B}}T)[1/S(k)+1]$. Evidently, (12) shows some similarity to the classical result if the energy $\hbar^2k^2/2m$ is replaced by its equipartition value. An important feature of the PPA is its ability to treat long-wavelength phonons correctly. It accomplishes this by including in $u(r)$ a slowly decaying long-ranged tail of the form

$$u(r)\sim\frac{1}{r^2}\qquad r\to\infty \tag{13}$$

which, as shown by Chester and Reatto [18], gives the exact long-ranged pair correlation of the ground-state wavefunction. The slow decay of $u(r)$ expressed by (13)

implies that the structure factor must vanish as $k \to 0$. More precisely, it can be shown [18] that at $T = 0$ $S(k)$ vanishes *linearly* with k (see figure 1(*a*)), according to

$$S(k) \sim \frac{\hbar k}{2mc_1} \quad (k \to 0). \tag{14}$$

We note that (11) and (14) together are consistent with the quantum compressibility rule (7). It is important to point out, however, that the PPA does not guarantee consistency between ϵ and $v(k)$, in the sense that ϵ and $v(k)$ do not necessarily satisfy (7) exactly. In other words, the speed of sound derived from ϵ differs from that derived from $v(k = 0)$ *via* (7). Therefore, in order to ensure that (7) *is* satisfied, we have *scaled* the PPA $v(k)$ by the factor $(2\epsilon' + \rho\epsilon'')/v(k = 0)$, which amounts to an increase in magnitude of roughly 20%. Figure 1(*b*) illustrates the resulting scaled $v(k)$.

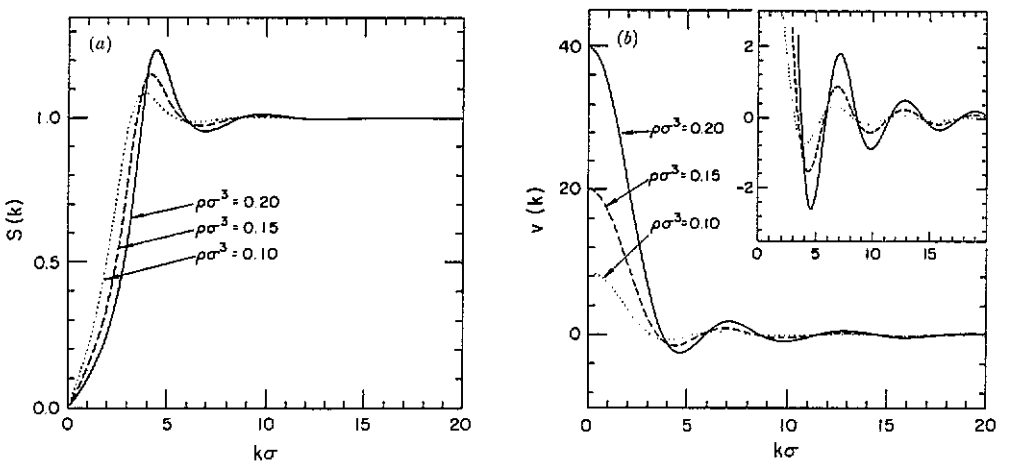

Figure 1. (*a*) PPA structure factor $S(k)$ versus k for the Bose hard-sphere liquid at reduced densities $\rho\sigma^3 = 0.10$ (dotted), 0.15 (broken), and 0.20 (full). (*b*) Corresponding *scaled* PPA quantum direct correlation function $v(k)$ versus k, used as input to the density-functional method (see text).

4. Freezing of the Bose hard-sphere liquid

Application of the density-functional method to freezing requires parametrization of the solid density $\rho_s(\boldsymbol{r})$. This involves first, the *choice* of a crystal structure and second, an assumption for the form of the density distribution about the lattice sites of the chosen crystal. As in previous studies of the classical hard-sphere system, we have assumed a perfect crystal with a simple Gaussian form

$$\rho_s(\boldsymbol{r}) \equiv \left(\frac{\alpha}{\pi}\right)^{3/2} \sum_{\boldsymbol{R}} e^{-\alpha|\boldsymbol{r}-\boldsymbol{R}|^2} \tag{15}$$

where α is a 'localization parameter' determining the width of the Gaussians centred on the lattice sites at positions $\boldsymbol{R}$. Although the Gaussian approximation has been

widely used in previous applications to *classical* hard spheres, its use here for *quantum* hard spheres requires some justification. It is suggested by the Green function Monte Carlo simulation of a Lennard-Jones model of ^{4}He of Whitlock *et al* [19], who examined the one-particle solid density and concluded that it was spherically symmetric about a given lattice site with only small positive deviations from Gaussian behaviour in the tail of the distribution. To our knowledge no such test has been performed for Bose hard spheres. Nevertheless, since we expect the hard-sphere and Lennard-Jones solids to exhibit rather similar behaviour, we judge these simulation results, and the ensuing results of the MWDA, to be reasonable justification for our use here of (15).

Once the solid density has been parametrized, application of the MWDA proceeds with (i) a computation of the weighted density, (ii) the minimization of the total solid energy with respect to the parametrized density, and (iii) the location of the liquid-solid transition. The weighted density $\hat{\rho}$ is computed from the Fourier-space form of (3),

$$\hat{\rho} = \rho_s + \frac{1}{\rho_s} \sum_{G \neq 0} \rho_G^2 w_G(\hat{\rho}) \tag{16}$$

where ρ_s is the average solid density, and ρ_G and w_G denote the Fourier components at reciprocal lattice vector (RLV) G of the solid density and the weight function, respectively. In the Gaussian approximation (15) the solid density has the simple Fourier component

$$\rho_G = \rho_s e^{-G^2/4\alpha}. \tag{17}$$

Substituting ρ_G (17) and w_G (6) into (16) now leads to

$$\hat{\rho}(\alpha, \rho_s) = \rho_s \left[1 + \frac{1}{2\epsilon'(\hat{\rho})} \sum_{G \neq 0} e^{-G^2/2\alpha} v(G; \hat{\rho}) \right] \tag{18}$$

an *implicit* relation for $\hat{\rho}$, which can be easily solved (at fixed ρ_s and α) by numerical iteration [20]. The iterative solution is illustrated graphically in figure 2(a), where the point of intersection between a weighted-density curve and the line of unit slope represents the fixed point to which the iterations converge. The resulting dependence of $\hat{\rho}$ on α is shown in figure 2(b) for the case of an FCC crystal. A key feature to note is the monotonic decrease of $\hat{\rho}$ with increasing α, implying that the more localized the atoms in the solid, the *lower* the density of the effective liquid whose correlation energy best approximates that of the solid. Once the weighted density has been computed from (19), the approximate correlation energy of the solid E_c^{MWDA} is given immediately by (2).

The ideal-gas energy E_{id}, can be formally expressed as

$$E_{\mathrm{id}} = \frac{\langle \psi_{\mathrm{id}} | T | \psi_{\mathrm{id}} \rangle}{\langle \psi_{\mathrm{id}} | \psi_{\mathrm{id}} \rangle} \tag{19}$$

where

$$T = -\frac{\hbar^2}{2m} \sum_{i=1}^{N} \nabla_i^2 \tag{20}$$

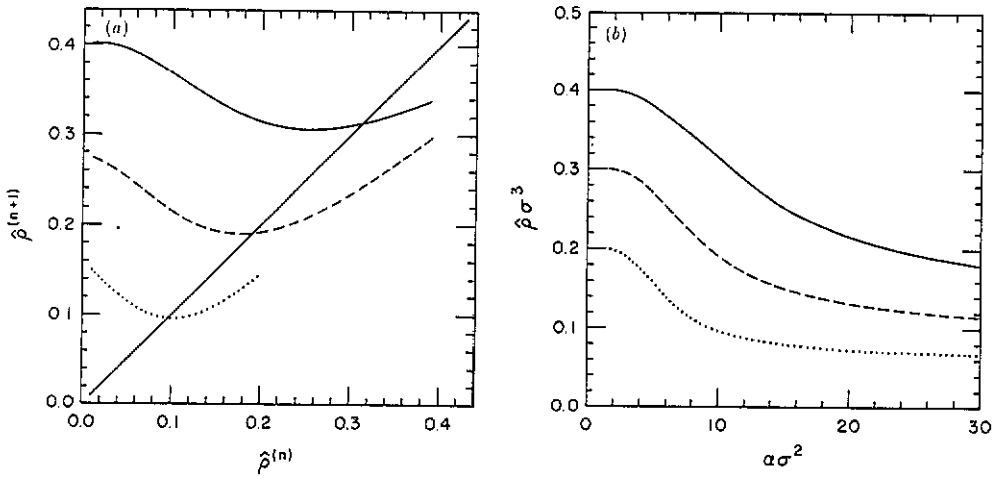

Figure 2. (*a*) Graphical illustration of the iterative solution of (18): $\hat{\rho}^{(n)}$ and $\hat{\rho}^{(n+1)}$ denote the weighted density at the nth and $(n+1)$th iterations. Curves are shown for the Bose hard-sphere FCC crystal at localization parameter $\alpha\sigma^2 = 10$ and reduced average solid densities $\rho_s\sigma^3 = 0.2$ (dotted), 0.3 (broken), and 0.4 (full). The point of intersection between a curve and the line of unit slope represents the fixed point to which the iterations converge. (*b*) Corresponding weighted densities versus localization parameter.

is the kinetic energy operator, and ψ_{id} the ground-state wavefunction of the non-interacting system. The density can be similarly expressed as

$$\rho(\boldsymbol{r}) = \frac{\langle\psi_{\mathrm{id}}|\sum_{i=1}^{N}\delta(\boldsymbol{r}-\boldsymbol{r}_i)|\psi_{\mathrm{id}}\rangle}{\langle\psi_{\mathrm{id}}|\psi_{\mathrm{id}}\rangle}. \tag{21}$$

Since for a non-interacting Bose system ψ_{id} takes the general form

$$\psi_{\mathrm{id}}(\boldsymbol{r}_1,\ldots,\boldsymbol{r}_N) = \prod_{i=1}^{N}\phi(\boldsymbol{r}_i) \tag{22}$$

where ϕ is a single-particle wavefunction, then

$$\rho(\boldsymbol{r}) = \frac{N|\phi(\boldsymbol{r})|^2}{\int \mathrm{d}\boldsymbol{r}\,|\phi(\boldsymbol{r})|^2} \tag{23}$$

and

$$E_{\mathrm{id}}[\rho] = \frac{\hbar^2}{2m}\int \mathrm{d}\boldsymbol{r}\,|\nabla\sqrt{\rho(\boldsymbol{r})}|^2. \tag{24}$$

In the case of *non-overlapping* Gaussians—a good approximation at densities near freezing—substitution of (15) into (24) leads to the particularly simple form [21]

$$E_{\mathrm{id}}/N \simeq \frac{3}{4}\frac{\hbar^2}{m}\alpha \tag{25}$$

identical to the form usually assumed in variational Monte Carlo (VMC) simulations [13–15]. The approximate total ground-state energy per particle of the solid is thus finally given by

$$E^{\mathrm{MWDA}}(\alpha,\rho_s)/N \simeq \frac{3}{4}\frac{\hbar^2}{m}\alpha + \epsilon(\hat{\rho}(\alpha,\rho_s)). \tag{26}$$

Next, E^{MWDA}/N is minimized with respect to α at *fixed* ρ_s. Figure 3 illustrates the minimization procedure, showing separately the behaviour of the correlation and ideal-gas energies. For simplicity, we have plotted for E_{id} only the linear approximation of (24), though this is strictly valid only for $\alpha\sigma^2 > 5$. Note that the ideal-gas energy increases with α, strongly *opposing* localization of the atoms about lattice sites; in contrast, the correlation energy falls off rapidly with α, strongly *favouring* localization. The competition between E_{id} and E_c may result—for sufficiently high ρ_s (as in figure 3)—in a minimum in the *total* energy at non-zero α, implying the existence of a mechanically stable solid [22]. Thermodynamic stability of the solid relative to the liquid is, however, determined by comparing the liquid and solid energies [23]. By now varying ρ_s and repeating the minimization procedure, the solid-phase energy curve (E/V versus ρ_s) is obtained. The result for the FCC crystal is shown together with the PPA liquid-phase energy curve in figure 4(*a*), where the crossing of the two curves confirms the occurrence of a freezing transition. Figure 4(*b*) shows the corresponding pressures [24]. Also shown in figure 4 are the VMC simulation data of Hansen *et al* [15] for the liquid and the FCC crystal. A more quantitative comparison between theory and simulation is given in table 1. The inset to figure 4(*a*) shows the dependence of the localization parameter α on the average solid density ρ_s, illustrating that an increase in the density naturally results in greater localization. The value of α at the solid coexistence density is directly related to the Lindemann parameter L, defined as the ratio of the RMS displacement of an atom from its lattice site to the nearest-neighbour distance in the solid at coexistence. For the FCC, HCP and BCC crystal structures, L is equal to $(3/\alpha a^2)^{1/2}$, $(3/2\alpha a^2)^{1/2}$ and $(2/\alpha a^2)^{1/2}$, respectively, where a is the lattice constant. Corresponding to figure 4, figure 5 shows the dependence of the weighted density (at the energy minimum) on the average solid density, demonstrating that $\hat{\rho}$ is always considerably *lower* than ρ_s.

Table 1. Energy per particle E/N (in units of $\hbar^2/m\sigma^2$) and pressure P (in units of $\hbar^2/m\sigma^5$) of the Bose hard-sphere FCC crystal at zero temperature over a range of average solid densities ρ_s.

$\rho_s\sigma^3$	E/N		P	
	Simulation†	MWDA	Simulation†	MWDA
0.244	8.8±0.1	9.98	3.5	3.22
0.27	10.5±0.1	11.44	4.8	4.33
0.3	12.6±0.1	13.34	6.8	6.00
0.35	16.8±0.2	16.99	11.3	9.80
0.4	21.9±0.2	21.37	18	15.30
0.5	35.5±0.3	32.78	40	34.19

† See [15]

The liquid–solid transition is finally located by constructing a common tangent to the liquid and solid energy curves, ensuring equality of the pressures and of the

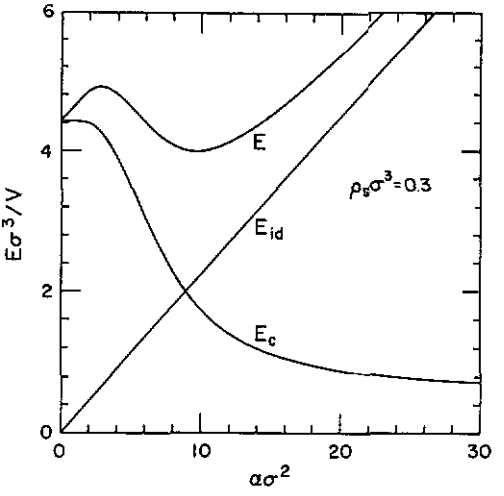

Figure 3. Ideal-gas, correlation, and total ground-state energies per volume (units of $\hbar^2/m\sigma^2$) versus localization parameter α for the Bose hard-sphere FCC crystal at reduced average solid density $\rho_s\sigma^3 = 0.3$, where E_{id} is the linear approximation of (25) and E_c is computed using the MWDA (2). The minimum in E/V versus α indicates a *mechanically* stable solid.

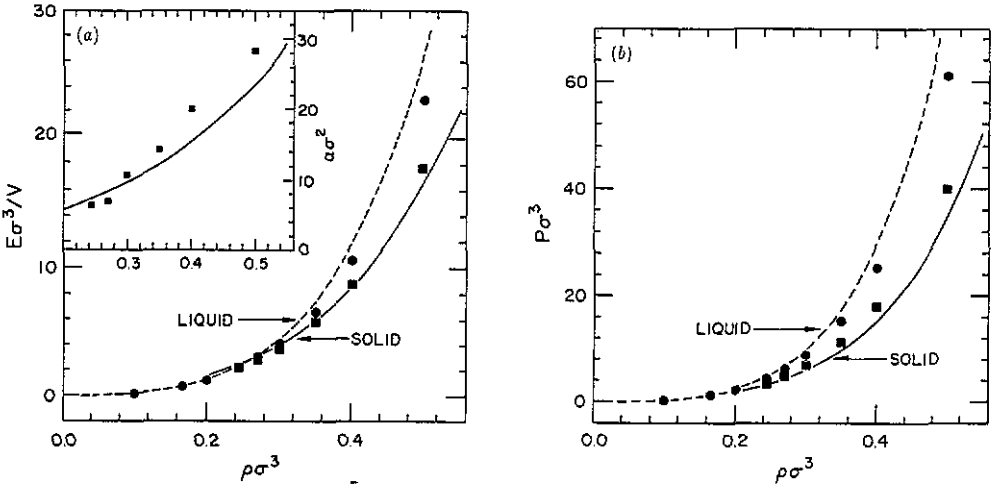

Figure 4. (*a*) Total ground-state energies per unit volume (units of $\hbar^2/m\sigma^5$) of the Bose hard-sphere liquid (from PPA) and FCC crystal (from MWDA). Circles and squares are VMC simulation data [15] for the liquid and solid phases, respectively. A common-tangent construction gives the densities of the liquid and solid at coexistence. The inset shows the density-dependence of the localization parameter α, illustrating the increase in localization with increasing density. (*b*) Corresponding ground-state pressures (units of $\hbar^2/m\sigma^5$).

chemical potentials in the two phases, and yielding the coexistence densities as the abscissae of the points of common tangency. The resulting freezing parameters are given in table 2 for FCC, HCP and BCC crystal structures, together with available VMC simulation data [15]. We have chosen to compare the theoretical results with the VMC

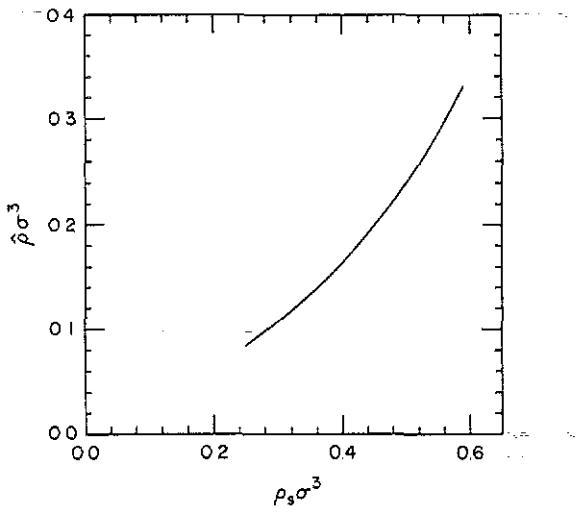

Figure 5. Weighted density $\hat{\rho}$ at the energy minimum versus average solid density ρ_s for the Bose hard-sphere FCC crystal, illustrating that the weighted density is always considerably lower than the average solid density.

simulation data, rather than with presumably more accurate Green function Monte Carlo (GFMC) data [26], because the liquid-state input to the theory was obtained by the same variational approach of the PPA. In any case, for hard spheres, the VMC and GFMC data generally differ by only a few percent [27].

Also shown in table 2 are the corresponding freezing parameters resulting from an analogous quantum extension of the RY second-order approximation [3] which is based on a *truncated* functional Taylor-series expansion of the correlation energy about the density ρ_l of a uniform reference liquid:

$$E_c^{RY}[\rho] \equiv E_c(\rho_l) + \left(\frac{\delta E_c}{\delta \rho(r)}\right)_l \int dr\, \Delta\rho(r) + \frac{1}{2}\int dr \int dr' \left(\frac{\delta^2 E_c}{\delta\rho(r)\delta\rho(r')}\right)_l \Delta\rho(r)\Delta\rho(r') \tag{27}$$

Table 2. Freezing parameters of the Bose hard-sphere system at zero temperature: average solid density ρ_s, liquid density ρ_l, change in density $\Delta\rho$, change in energy per particle $\Delta(E/N)$ (units of $\hbar^2/m\sigma^2$), Lindemann parameter L, and c/a ratio for the HCP crystal [25].

	$\rho_s\sigma^3$	$\rho_l\sigma^3$	$\Delta\rho\sigma^3$	$\Delta(E/N)$	L	c/a
Simulation†						
FCC	0.25±0.02	0.23±0.02	0.02	1.28	0.27	
MWDA						
FCC	0.284	0.246	0.038	2.668	0.240	
HCP	0.284	0.246	0.038	2.688	0.240	1.629
BCC	0.280	0.247	0.033	2.338	0.249	
RY						
FCC	0.315	0.278	0.037	3.183	0.233	
HCP	0.318	0.279	0.039	3.330	0.234	1.642
BCC	0.317	0.280	0.037	3.234	0.249	

† See [15]

where $\Delta\rho(\boldsymbol{r}) \equiv \rho_s(\boldsymbol{r}) - \rho_l$, and the subscript l indicates evaluation at $\rho(\boldsymbol{r}) = \rho_l$. Although in a solid $\Delta\rho(\boldsymbol{r})$ varies rapidly compared with ρ_l, the third- and higher-order terms in the expansion are ignored, on the original grounds that the higher-order direct correlation functions are generally unknown. Application to freezing requires minimization, with respect to the Gaussian solid density, of the grand potential difference per unit volume between the solid and liquid phases $\Delta\Omega/V$ at the *same* chemical potential μ:

$$\Delta\Omega/V \equiv (\Omega_s - \Omega_l)/V \equiv (E_s - E_l)/V - \mu(\rho_s - \rho_l). \tag{28}$$

From (5), (17), (25), and (27), the approximation for (28) now takes the form [28]

$$\Delta\Omega^{\mathrm{RY}}(\alpha, \rho_s, \rho_l)/V \simeq \frac{3}{4}\frac{\hbar^2}{m}\alpha\rho_s + \frac{1}{2}v(G=0;\rho_l)(\rho_s - \rho_l)^2 + \frac{1}{2}\rho_s^2 \sum_{G\neq 0} \mathrm{e}^{-G^2/2\alpha} v(G;\rho_l) \tag{29}$$

which is to be minimized with respect to both α and ρ_s at fixed ρ_l. Equality of the liquid and solid pressures is finally ensured by variation of ρ_l until the minimum occurs at $\Delta\Omega^{\mathrm{RY}}/V = 0$. The minimization procedure is illustrated in figures 6 and 7.

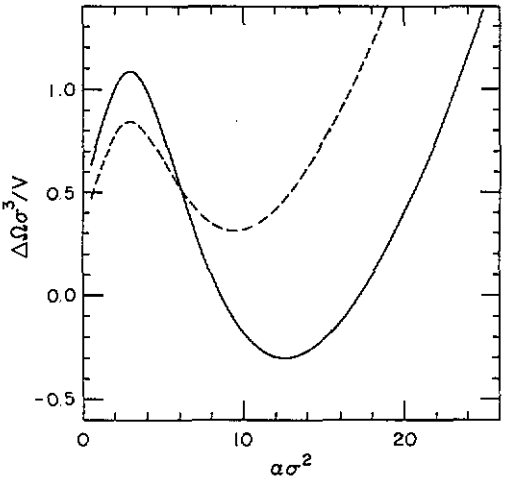

Figure 6. RY second-order approximation for the grand potential difference per unit volume $\Delta\Omega/V$ versus localization parameter α for the Bose hard-sphere FCC crystal at reduced average solid and uniform liquid densities $\rho_s\sigma^3 = 0.35$, $\rho_l\sigma^3 = 0.30$ (full) and $\rho_s\sigma^3 = 0.30$, $\rho_l\sigma^3 = 0.25$ (broken). A minimum indicates a mechanically stable solid.

5. Discussion

From figure 4 and table 1, it is seen that the FCC-crystal energies and pressures given by the MWDA are quite close to the VMC simulation data, differing by at most 15%. The deviation of the PPA liquid-phase $\epsilon(\rho)$ from simulation seen at higher densities in

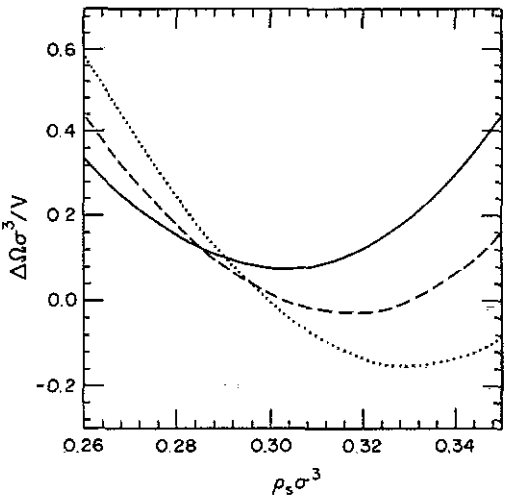

Figure 7. RY second-order approximation for the grand potential difference per unit volume $\Delta\Omega/V$ (minimized with respect to localization parameter α) versus average solid density ρ_s at reduced uniform liquid densities $\rho_l\sigma^3 = 0.27$ (full), 0.28 (broken), and 0.29 (dotted). A minimum at $\Delta\Omega/V = 0$ implies liquid–solid coexistence.

figure 4(a) can be attributed to the increasing inaccuracy of the HNC approximation with increasing density. The actual deviation is found to be 2–4% at $\rho\sigma^3 = 0.2$, and about 10% at $\rho\sigma^3 = 0.3$. In practice, however, this high-density deviation is *not significant, since the* MWDA *requires the liquid-state input only at the weighted* density (see (18)), which near freezing is sufficiently low (see figure 5) that the PPA and VMC energies actually agree to within the Monte Carlo statistical error.

Taking into consideration the extreme sensitivity of the coexistence densities—as determined by the common-tangent construction—to the accuracy of the solid-phase energies, we view the comparison between the MWDA freezing parameters and simulation (table 2) as quite favourable. We note first that the predicted solid and liquid coexistence densities are a little too high, by 14% and 7%, respectively. The predicted *change* in density is significantly higher than the simulation value, which itself is probably an underestimate [29]. The Lindemann parameter, however, a quite sensitive test of a freezing theory, is underpredicted by only 11%. This discrepancy, as well as that in the change in energy per particle, can be at least partly attributed to the overprediction of the solid coexistence density.

In comparison, the freezing parameters given by the RY second-order approximation are seen to be in generally poorer agreement with simulation. The solid and liquid densities are too high by 26% and 21%, respectively, and the Lindemann parameter is too low by 14%. It is worth noting, however, that the Lindemann parameter is here in much closer agreement with simulation than in the case of the *classical* hard-sphere system, where the RY prediction is too small by a factor of more than two [30]. Although it might be argued from this result that the second-order approximation is better justified for a quantum solid where the local density varies less rapidly and sharply, it should be appreciated that the ratio of peak to average solid density is still considerable (roughly 20) in the quantum solid at freezing.

The Lindemann parameter is of particular significance to the physical nature of the freezing transition. Its value predicted by the MWDA for Bose hard spheres ($L = 0.240$,

from table 2) is more than twice the corresponding prediction for classical hard spheres ($L = 0.097$, from [7]), in general agreement with simulation [19]. In the theory, the larger quantum value is a direct consequence of the relatively strong variation of the ideal-gas and correlation energies with the localization parameter (figure 3 of this paper should be compared with figure 2 of [7]). The linear increase of E_{id} with α near freezing is much more rapid than the corresponding logarithmic increase of the ideal-gas free energy in the classical system [7,8]. Consequently, if the *total* energy is to have a minimum, then E_c must decrease much more rapidly with α than its classical counterpart, the excess free energy. From (19), it is seen that the rate of variation of $\hat{\rho}$, and hence of E_c, with α is determined by the RLV magnitudes G, and that the variation is more rapid the lower the G, or equivalently, the lower the average density of the solid. Whether E_c actually decreases with α, however, depends crucially on the Fourier components of the DCF $v(G)$. Evidently E_c *does* decrease with the $v(G)$ used here, and the result is a minimum of the total energy at a much lower value of α (weaker localization), *and* necessarily at a much lower density, than in the classical system.

The choice of crystal structure evidently has only a minor effect on the values of the freezing parameters, reflecting the fact that the predicted energies of the different structures are extremely close, actually differing by less than 0.5% over the full density range. Indeed, on the scale of figure 4(a) the energy curves would be practically indistinguishable. The similarity of the two close-packed structures is not unexpected, considering that the FCC and ideal HCP structures differ in real space only in third-nearest-neighbour coordination. This similarity has been previously observed in simulations both of a Lennard-Jones model of ^{4}He [31] and of *classical* hard-spheres [32]. The similarity of the BCC structure to the close-packed structures is more interesting, and somewhat surprising given the significant differences between BCC and close-packed symmetries, reflected in the theory by the different sets of RLV entering in (18) and (29). It is in sharp contrast to the classical hard-sphere system, where both density-functional theory and simulation predict the free energy of the BCC crystal to be always significantly higher than that of the FCC crystal [33]. It may indicate a smaller sensitivity to structure in the quantum system, resulting from the larger RMS atomic displacements in the quantum solid. To our knowledge, there exist no simulation results for freezing of the Bose hard-sphere liquid into a BCC crystal with which to compare our prediction (but see [34]).

6. Summary and conclusions

In summary, we have proposed a general extension of the modified weighted-density approximation from classical systems to quantum systems at zero temperature, which requires as input only the correlation energy per particle and the direct correlation function of the *uniform* liquid. We have applied the theory to freezing of the Bose hard-sphere liquid, taking the liquid-state information from the paired phonon analysis. The resulting solid-phase energies and freezing parameters generally compare well with available simulation data, although the result for the density change upon freezing is somewhat too high. An analogous extension of the Ramakrishnan–Yussouff second-order approximation leads to freezing parameters in generally poorer agreement with simulation. The large magnitude of the quantum Lindemann parameter, as compared to its classical counterpart, can be understood as a consequence of the relatively high

sensitivity to localization of the ideal-gas and correlation energies in the quantum system. Interestingly, the BCC crystal is found to exhibit freezing properties almost identical to those of the close-packed FCC and HCP crystals, a prediction which we suggest may be directly tested by simulation.

The theory presented here appears to be a satisfactory extension of the classical density-functional method to quantum freezing. It is important to mention, however, that the freezing predictions are very sensitive to the liquid-state input, and that scaling of the PPA $v(k)$, to ensure that the quantum compressibility rule is satisfied, is crucial to the favourable agreement with simulation. Indeed, with the unscaled PPA $v(k)$ as input the solid is found to be always unstable. Although the theory has been demonstrated here to be successful for *some* liquid-state input, it will be important in future to test it further by using even more accurate input, and also by applying it to other problems. In addition to freezing, the theory may prove useful in studying other bulk-phase phenomena, such as solid–solid transitions and elasticity phenomena. It may also be applied to other simple systems, such as Fermi hard spheres or Lennard-Jones models of ^{3}He and ^{4}He [19,26]. Preliminary attempts suggest that the theory cannot be *directly* applied to Lennard-Jones systems at zero temperature, where the variation with density of the liquid-state energy is not sufficiently rapid to yield a weighted density low enough to stabilize the solid. Such systems may be treated, however, using perturbation theory with the hard-sphere liquid taken as the reference system [19,26]. Finally, an important problem, which we are currently studying, is the extension of the theory to quantum systems at *finite* temperatures.

Acknowledgments

This work was supported by NSF Grant No DMR-8715590. One of us (ARD) gratefully acknowledges partial support from the Natural Sciences and Engineering Research Council of Canada. The computations were performed using the Cornell National Supercomputer Facility, a resource of the Center for Theory and Simulation in Science and Engineering (Cornell Theory Center) which receives major funding from the National Science Foundation and IBM Corporation, in addition to support from New York State and members of the Corporate Research Institute.

References

[1] For reviews of the density-functional method in the context of classical fluids, see
Oxtoby D W 1990 *Liquids, Freezing, and the Glass Transitions (Les Houches Session 51)* ed J P Hansen, D Levesque and J Zinn-Justin (New York: Elsevier)
Baus M 1990 *J. Phys.: Condens. Matter* **2** 2111
Evans R 1989 *Liquids at Interfaces (Les Houches Session 48)* ed J Charvolin, J F Joanny and J Zinn-Justin (New York: Elsevier); 1979 *Adv. Phys.* **28** 143
Baus M 1987 *J. Stat. Phys.* **48** 1129
Haymet A D J 1986 *Prog. Solid State Chem.* **17** 1

[2] Hansen J-P and McDonald I R 1986 *Theory of Simple Liquids* 2nd edn (London: Academic)
Barker J A and Henderson D 1976 *Rev. Mod. Phys.* **48** 587

[3] Ramakrishnan T V and Yussouff M 1979 *Phys. Rev.* B **19** 2775
Haymet A D J and Oxtoby D W 1981 *J. Chem. Phys.* **74** 2559

[4] McCoy J D, Rick S W and Haymet A D J 1990 *J. Chem. Phys.* **92** 3034, 3040; 1989 *J. Chem. Phys.* **90** 4622

[5] Senatore G and Pastore G 1990 *Phys. Rev. Lett.* **64** 303

[6] For an early extension of the Kirkwood-Monroe theory (a precursor to modern density-functional theory) to freezing of ^{4}He see
Miller M D, Mullin W J and Guyer R A 1978 *Phys. Rev.* B **18** 3189
[7] Denton A R and Ashcroft N W 1989 *Phys. Rev.* A **39** 4701
[8] Curtin W A and Ashcroft N W 1985 *Phys. Rev.* A **32** 2909; 1986 *Phys. Rev. Lett.* **56** 2775
[9] Chang C C and Campbell C E 1977 *Phys. Rev.* B **15** 4238; Jackson H W and Feenberg E 1961 *Ann. Phys.* **15** 266
[10] Denton A R, Nielaba P, Runge K J and Ashcroft N W 1990 *Phys. Rev. Lett.* **64** 1529
[11] Hohenberg P and Kohn W 1964 *Phys. Rev.* **136** B864
[12] McMillan W L 1965 *Phys. Rev.* A **138** 442
[13] Schiff D and Verlet L 1967 *Phys. Rev.* **160** 208
[14] Hansen J-P and Levesque D 1968 *Phys. Rev.* **165** 293
[15] Hansen J-P, Levesque D and Schiff D 1971 *Phys. Rev.* A **3** 776
[16] Whitlock P A and Vitiello S private communication
[17] Krotscheck E 1986 *Phys. Rev.* B **33** 3158
[18] Chester G V and Reatto L 1966 *Phys. Lett.* **22** 276
[19] Whitlock P A, Ceperley D M, Chester G V and Kalos M H 1979 *Phys. Rev.* B **19** 5598
[20] Two important practical points concerning the numerical solution of (18): first, we computed $\epsilon(\rho)$ and $v(k,\rho)$ at discrete densities and wave vectors in the ranges $0 < \rho\sigma^3 < 0.4$ (at intervals of 0.01) and $0 < k\sigma < 30$ (at intervals of about 0.1). We then fitted $\epsilon(\rho)$ by a fourth-order polynomial, and for $v(k,\rho)$ simply linearly interpolated between points. Second, for the values of α relevant near freezing we find that 10 RLV shells, a given shell including all RLV of the same magnitude, is quite sufficient to ensure convergence of the sum in (18).
[21] Note that the ideal-gas energy per particle in (25) is precisely equal to the ground-state kinetic energy of a three-dimensional quantum mechanical harmonic oscillator with angular frequency $\omega = \hbar\alpha/m$, a direct consequence of the Gaussian approximation assumed for the density.
[22] A similar competition is seen in the classical system between the ideal-gas and excess free energies. Note, however, that whereas the classical hard-sphere free energy is purely entropic, the quantum hard-sphere ground-state energy is purely kinetic.
[23] From (26), it is easily shown that E^{MWDA}/N initially increases with α, implying that the liquid phase (at $\alpha = 0$) is always at least metastable.
[24] The pressures listed in table 1 were obtained from the relation $P = \rho^2\partial(E/N)/\partial\rho$, the derivative being evaluated numerically.
[25] For the HCP structure, the c/a ratio was treated as an additional variational parameter. Note that its optimum value is very close to the ideal value $c/a = (8/3)^{1/2}$ for close-packed hard spheres.
[26] Kalos M H, Levesque D and Verlet L 1974 *Phys. Rev.* **9** 2178
[27] Note that for Lennard-Jones models of ^{4}He, VMC and GFMC simulation results may differ by as much as 20% (see [19]).
[28] In deriving (29), we have used the relation $(\delta E_c/\delta\rho(\mathbf{r}))_l = \mu$, since the ideal liquid chemical potential (obtained from (24)) is identically zero.
[29] Extrapolation to zero temperature of recent, and very accurate, finite-temperature Path-Integral Monte Carlo results (Runge K J and Chester G V 1988 *Phys. Rev.* B **38** 135) suggests that the actual density change may be *at least* a factor of two *lower* than the value sited in table 2.
[30] For accurate results of the RY theory applied to the freezing of *classical* hard spheres, see Barrat J-L, Hansen J-P, Pastore G and Waisman E M 1987 *J. Chem. Phys.* **86** 6360; Curtin W A 1988 *J. Chem. Phys.* **88** 7050
[31] Whitlock P A, Ceperley D M, Chester G V and Kalos M H 1981 *Phys. Rev.* B **21** 999
[32] Frenkel D and Ladd A J C 1984 *J. Chem. Phys.* **81** 3188
[33] Curtin W A and Runge K 1987 *Phys. Rev.* A **35** 4755
[34] In VMC simulations of Lennard-Jones models of solid ^{3}He and ^{4}He the ground-state energies of BCC and HCP crystals have been found to differ by less than one percent of the kinetic energy (Hansen J-P 1969 *Phys. Lett.* **30A** 214). Furthermore, experimentally, both ^{3}He and ^{4}He may exist near zero temperature in either the BCC or HCP structure, depending upon the pressure. See, for example, Wilks J 1967 *The Properties of Liquid and Solid Helium* (Oxford: Clarendon)